Uncoupling of sustained MAMP receptor signaling from early outputs in an Arabidopsis endoplasmic reticulum glucosidase II allele

Xunli Lu[a], Nico Tintor[a], Tobias Mentzel[b], Erich Kombrink[a], Thomas Boller[b], Silke Robatzek[a], Paul Schulze-Lefert[a,1], and Yusuke Saijo[a,1]

[a]Department of Plant Microbe Interactions, Max Planck Institute for Plant Breeding Research, 50829 Cologne, Germany; and [b]Botanical Institute, University of Basel, 4056 Basel, Switzerland

Edited by Frederick M. Ausubel, Harvard Medical School, Boston, MA, and approved October 22, 2009 (received for review July 15, 2009)

Recognition of microbe-associated molecular patterns (MAMPs), conserved structures typical of a microbial class, triggers immune responses in eukaryotes. This is accompanied by a diverse set of physiological responses that are thought to enhance defense activity in plants. However, the extent and mechanisms by which MAMP-induced events contribute to host immunity are poorly understood. Here we reveal Arabidopsis *priority in sweet life4* (*psl4*) and *psl5* mutants that are insensitive to the bacterial elongation factor (EF)-Tu epitope elf18 but responsive to flagellin epitope flg22. PSL4 and PSL5, respectively, identify β- and α-subunits of endoplasmic reticulum-resident glucosidase II, which is essential for stable accumulation and quality control of the elf18 receptor EFR but not the flg22 receptor FLS2. We notice that EFR signaling is partially and differentially impaired without a significant decrease of the receptor steady-state levels in 2 weakly dysfunctional *gIIα* alleles, designated *psl5*-1 and *rsw3*. Remarkably, *rsw3* plants exhibit marked supersusceptibility against a virulent bacterial phytopathogen despite nearly intact coactivation of MAPKs, reactive oxygen species, ethylene biosynthesis, and callose deposition in response to elf18, demonstrating that these signaling outputs alone are insufficient to mount effective immunity. However, *rsw3* plants fail to maintain high transcript levels of defense-promoting *WRKY*, *PR1, and PR2* genes at late time points (4 to 24 h) after elf18 elicitation. This points to an unexpected separation between initial and sustained activation of EFR-mediated signaling in the absence of proper glucosidase II-mediated endoplasmic reticulum quality control. Our findings strongly suggest the importance of sustained MAMP receptor signaling as a key step in the establishment of robust immunity.

EFR | ER quality control | LRR RLK | plant immunity

Activation of pattern recognition receptors (PRRs) upon microbe-associated molecular pattern (MAMP) perception leads to an enhanced state of immunity that limits invasion and propagation of potential microbial intruders, termed MAMP-triggered immunity (MTI) (1). MTI is associated with the activation of a stereotypical set of cellular responses that occur from seconds/minutes to hours/days upon elicitation. Early responses including ion fluxes across the plasma membranes, reactive oxygen species (ROS) spiking, and MAPK activation are generally followed by ethylene production, transcriptional reprogramming, metabolomic changes, and callose deposition (2–6). As recognition of different MAMPs triggers largely similar host responses, it is presumed that distinct PRR pathways converge on those signaling outputs. However, the physiological relevance of these MTI-associated events for overall host defense activity and the mechanisms by which a single receptor regulates signaling pathways leading to such diverse outputs remain elusive.

Because prolonged defense activation results in growth retardation, repression of abiotic stress responses, and/or cell death in plants (5, 7–9), plants evolved specific mechanisms conferring stringent control on abundance and activation/deactivation states of immune receptors. As for intracellular immune receptors containing nucleotide binding and leucine-rich repeat (LRR) domains, a widespread class of disease resistance proteins, the importance of protein abundance control via cytosolic HSP90/SGT1/RAR1 chaperone complexes has been well documented (10). The requirement of HSP90 and SGT1 has been demonstrated for nucleotide binding/LRR protein functions in vertebrate innate immunity (11). However, it is still unclear whether these chaperones are engaged in postactivation signaling and/or desensitization of the client immune receptors.

In eukaryotic cells, folding and maturation of the majority of membrane-localized proteins occur in the endoplasmic reticulum (ER), where elaborate quality control ensures that only correctly folded proteins are delivered to their functional sites. A major branch of endoplasmic reticulum quality control (ERQC) relies on Asn (N)-linked glycosylation on the client proteins (12–14). N-glycosylation is catalyzed by the oligosaccharyltransferase (OST) complex that transfers a preassembled glycan chain ($Glc_3Man_9GlcNAc_2$) to N residues in the sequon N-X-Ser/Thr (X = any amino acid except Pro) of acceptor proteins. Subsequent trimming of terminal glucose residues by glucosidase I (GI) and glucosidase II (GII) produces mono-glucosylated glycans ($Glc_1Man_9GlcNAc_2$) on the client proteins, thereby facilitating their recognition and folding by the ER-resident chaperons calnexin (CNX) and calreticulin (CRT). Following this folding attempt, GII-mediated removal of the outermost glucose residues releases $Man_9GlcNAc_2$-conjugated client proteins from the chaperones. Properly folded proteins are transferred to their functional sites, whereas unfolded proteins are recognized by UDP-glucose:glycoprotein glucosyltransferase (UGGT). UGGT attaches a glucose residue to N-linked $Man_9GlcNAc_2$ glycans of client proteins, and then facilitates the client proteins to enter reiterated rounds of CNX/CRT-assisted folding (CNX/CRT cycle) (12–14). Severe loss of OST, GI, or GII function causes lethality in plants as well as in animals (12, 15–18). Arabidopsis plants carrying weak alleles of these genes are viable, but show phenotypic alterations under abiotic stress conditions (16, 18), suggesting a rate-limiting role of the N-glycosylation pathway for the adaptation to these stresses.

In Arabidopsis, the LRR receptor-like kinases (RLKs) EFR and FLS2, respectively, act as PRRs for the bacterial epitopes elf18 and flg22 (19, 20). Here we present evidence that Arabidopsis GII is required for stable accumulation and function of EFR but not of FLS2. We further show that EFR signaling outputs are partially and differentially impaired in weakly de-

Author contributions: X.L., P.S.-L., and Y.S. designed research; X.L., N.T., T.M., and Y.S. performed research; X.L., N.T., E.K., S.R., and Y.S. contributed new reagents/analytic tools; X.L., N.T., T.M., T.B., and Y.S. analyzed data; and X.L., P.S.-L., and Y.S. wrote the paper.

The authors declare no conflict of interest.

This article is a PNAS Direct Submission.

[1]To whom correspondence may be addressed. E-mail: saijo@mpiz-koeln.mpg.de or schlef@mpiz-koeln.mpg.de.

This article contains supporting information online at www.pnas.org/cgi/content/full/0907711106/DCSupplemental.

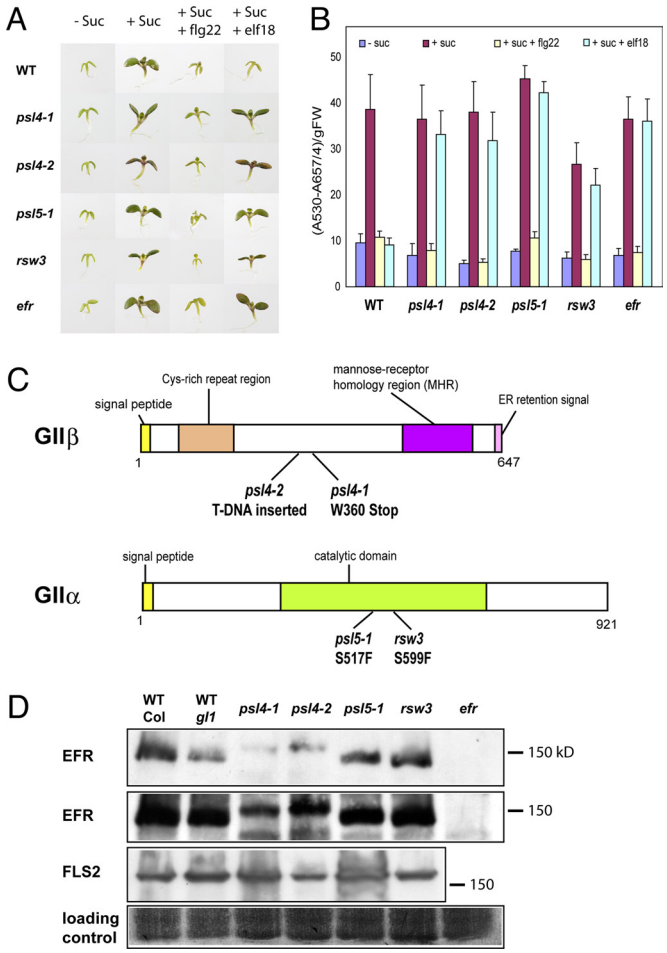

Fig. 1. PSL4 and PSL5, respectively, identify GII β- and α-subunits that are required for EFR but not FLS2 function. (*A*) WT (Col-0) and *gII* mutant seedlings grown in the absence of sucrose (− *Suc*) or presence of 100 mM sucrose (+ *Suc*) without or with 1 μM flg22 (+ *flg22*) or elf18 (+ *elf18*). (*B*) Anthocyanin content of seedlings grown as described in *A*, including the SD. (*C*) Schematic description of the structure of GII β- and α-subunits (647 and 921 aa residues, respectively). Positions of changes in the amino acid sequences in the mutant alleles are shown (*Bottom*). (*D*) Immunoblot analysis of protein extracts from 2-week-old nonelicited plants with the indicated antibodies. As for EFR, a long exposed blot is also shown in the second panel. A Coomassie blue-stained blot is presented to verify equal loading. Positions of molecular weight markers are shown (*Right*).

fective *gII* alleles, providing a genetic tool to dissect postrecognition signaling events of EFR. In a previously isolated *gII*α allele, designated *rsw3*, EFR-mediated immunity to a bacterial pathogen is compromised despite the coactivation of ROS, MAPKs, ethylene biosynthesis, and callose deposition. However, activation of defense gene expression is not maintained in the mutant, pointing to an unexpected role of sustained activation of PRR signaling for effective immunity.

Results

Identification of Arabidopsis *priority in sweet life* (*psl*) Mutants That Are Insensitive to elf18 but Sensitive to flg22. Exposure to different microbes or MAMPs leads to repression of flavonoid accumulation in plants (8, 9), at the cost of the adaptation to various abiotic stresses (21). For example, sucrose stress-induced anthocyanin accumulation is blocked in the presence of flg22 or elf18 in Arabidopsis seedlings (Fig. 1 *A* and *B*) (22). We have screened more than 60,000 ethyl methanesulfonate-mutagenized M_2 seedlings for individuals that are defective in this negative crosstalk. Our screens revealed >50 *psl* mutants that show derepressed sucrose-induced anthocyanin accumulation in the presence of elf18 but retain WT-like responsiveness to flg22 (Fig. 1 *A* and *B*). The results indicate the existence of separate genetic requirements for the function of the corresponding 2 PRRs despite their highly related overall structure (1). The *psl* mutants are classified into at least 5 complementation groups, including novel *efr* alleles as well as nonreceptor *psl1*, *ps2*, *psl4*, and *psl5* mutants (Fig. 1 *A* and *B*) (22). We described elsewhere that PSL1 and PSL2 identify CRT3 (AT1G08450) and UGGT (AT1G71220), respectively (22).

PSL4 and PSL5, Respectively, Define β- and α-Subunits of the ER-Resident GII that Is Indispensable for Biogenesis of EFR but Not FLS2. We identified *PSL4* by positional cloning of the *psl4–1* allele and subsequent recovery of another independent allele, *psl4–2* (Fig. 1*C* and Fig. S1*A*). *PSL4* encodes the deduced β-subunit of the ER lumen enzyme GII (At5g56360), the only homologue annotated in the Arabidopsis genome (Fig. 1*C*). Consistent with the predicted truncations in the large *C*-terminal portion of the protein, both *psl4* mutants fail to accumulate the encoded protein (Fig. S1*B*). Besides, *psl4–1* plants transformed with a genomic *GII*β copy fully complement the *psl* phenotype (Fig. S1 *D* and *E*). Thus, we conclude that GIIβ is required for EFR-mediated anthocyanin repression.

GII has been shown in animal cells to act as a heterodimer of 2 subunits, α and β: GIIα mediates the catalytic activity of the enzyme whereas GIIβ directly interacts with and holds GIIα in the ER through its ER retention signal (23, 24). In view of the functional interdependence between the 2 GII subunits, we searched for *gIIa* alleles in the remaining *psl* mutants. A single gene is annotated to encode a GIIα homologue (At5g63840) in Arabidopsis. Sequence analysis of the genomic locus revealed a *gII*α allele, *psl5–1*, carrying a point substitution in the catalytic domain (Fig. 1*C*). In addition, we tested MAMP responses in a previously isolated *gII*α allele, *rsw3*, that results in another amino acid substitution within the catalytic domain. The *rsw3* allele has been described to show a swollen root phenotype associated with defects in cellulose biosynthesis at high temperature (30 °C) (16). At the permissive temperature of approximately 22 °C, at which *rsw3* roots develop indistinguishably from WT, both *gII*α alleles exhibit derepressed anthocyanin accumulation in the presence of elf18 but not flg22 (Fig. 1 *A* and *B*). Both Ser residues substituted in the *gII*α alleles are invariant in GIIα orthologues not only from other plants but also in mouse and *Schizosaccharomyces pombe* (16). We verified cosegregation of the identified substitutions and elf18 hyposensitivity in both *gII*α alleles (Tables S1 and S2). Accumulation of the GIIβ subunit remains unaffected in these *gII*α plants (Fig. S1*B*). Thus, although it is currently unknown whether and how these substitutions influence GII catalytic activity *in planta*, our genetic evidence indicates that both GIIα and GIIß subunits are required for EFR but not FLS2 function.

In parallel, we have shown selective requirements of the ER-resident CRT3, UGGT, and an OST subunit for stable accumulation and thus function of EFR but not of FLS2 (22). Immunoblot analysis of protein extracts derived from nonelicited plants revealed that steady-state levels of EFR are greatly reduced without a significant decrease in its mRNA levels in the presence of *psl4* alleles (Fig. 1*D* and Fig. S1*C*). This is accompanied by a severe defect in EFR-dependent binding capacity to the ligand elf26 (equivalent to elf18; Fig. S2). Thus, GII seems to promote stable EFR accumulation at a posttranscriptional step during its biogenesis. Together, this is in accordance with the notion that GII acts in concert with CRT3 and UGGT in an ER N-glycosylation pathway that defines the biogenesis route of EFR. An apparently high-molecular-weight form of EFR detected in *psl4* plant lysates (Fig. 1*D*) might represent an under-trimmed N-glycan-conjugated form(s) of the receptor, presumably as a consequence of low ER GII activity in the mutants. Importantly, the abundance, apparent size, and specific ligand binding of FLS2 remain unaffected in the *psl4* plants (Fig. 1*D* and Fig. S2), again pointing to the specific

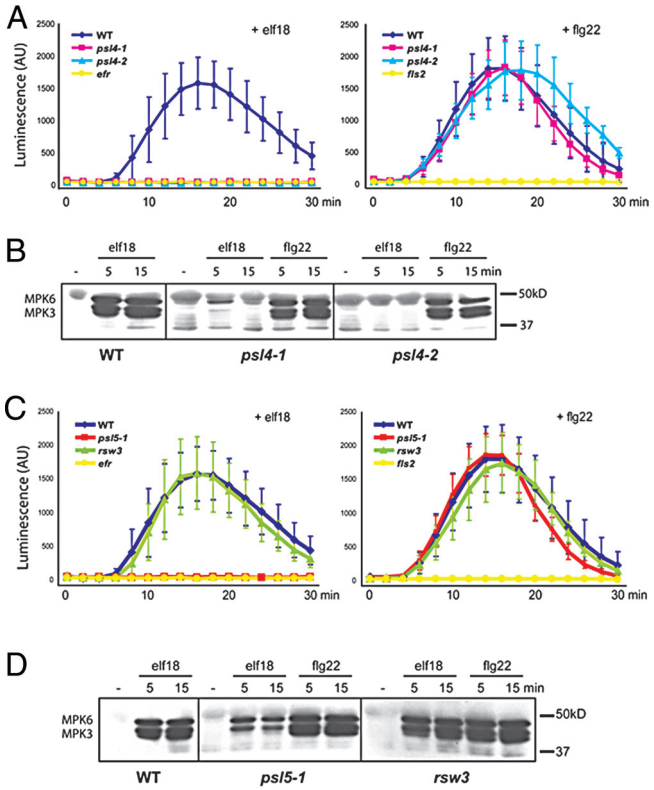

Fig. 2. MAMP-induced ROS spiking and MAPK activation in *gII* mutant plants. (*A* and *C*) ROS spiking triggered in leaf discs of the WT, *efr*, *fls2*, and *gII* plants at 100 nM elf18 (*Left*) or flg22 (*Right*), including the SD. (*B* and *D*) MAPK activation in WT and *gII* seedlings upon application of water for 5 min (−) or 1 μM elf18 or flg22 for the indicated times. Positions of active MPK3 and MPK6 forms (*Left*) and molecular weight markers (*Right*) are indicated.

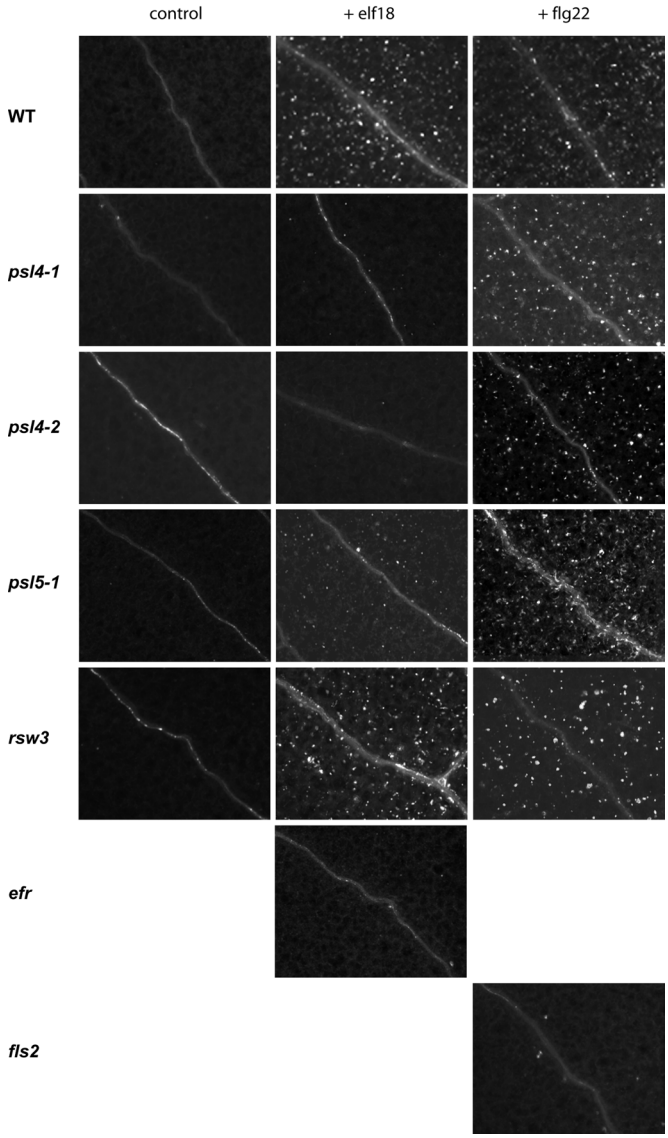

Fig. 3. MAMP-induced callose deposition in *gII* mutant plants. Callose deposits stained with aniline blue in the cotyledons of WT, *efr*, *fls2*, and *gII* seedlings treated with water (−) or 2 μM elf18 or 1 μM flg22 for 24 h. Representative photographs of more than 12 seedlings tested per sample are shown.

requirements of a GII-mediated ERQC step for EFR but not FLS2 biogenesis.

EFR-Mediated Signaling Is Severely Impaired in Strong *psl4* (*gIIβ*) Mutant Plants. We next tested possible defects in characteristic MAMP-induced responses in *psl4* plants. The observed decrease in EFR abundance, a complete size shift of the receptor (Fig. 1*D*), and lack of GIIβ detection (Fig. S1*B*) demonstrate that these plants carry strongly defective *gII*β alleles. Both *psl4* plants fail to trigger ROS spiking and MAPK activation in response to elf18 (Fig. 2 *A* and *B*). These plants are also defective in PMR4/GSL5-dependent callose deposition in the presence of elf18 (Fig. 3). In addition, elf18-induced ethylene production is hardly detectable in *psl4–1* plants (Fig. S3). However, both *psl4* plants retain WT-like responsiveness to flg22 in all of the assays (Fig. 2 *A* and *B*, Fig. 3, and Fig. S3), thus making it unlikely that the machineries directly executing these responses are dysfunctional per se.

EFR-Mediated Signaling Is Partially and Differentially Impaired in Weak *psl5* (*gIIα*) Mutant Plants. We noticed that EFR accumulates at WT-like levels in the absence or presence of elf18 elicitation in both *gII*α alleles (Fig. 1*D* and Fig. S4*A*) that are defective in elf18-dependent anthocyanin repression (Fig. 1 *A* and *B*). However, EFR-dependent ligand binding activity is greatly and slightly reduced in *psl5–1* and *rsw3* plants, respectively (Fig. S4*B*). This strongly suggests that dysfunction of GIIα perturbs EFR function per se, likely through improper folding of EFR. This is a unique example in plants indicating that the α- and β-subunits of GII indeed act in concert for an ERQC client protein. As one function of GIIβ is to engage into the ER-retrieval mechanism the α-subunit that lacks both a transmembrane segment and a known ER retention motif (Fig. 1*C*) (23, 24), it is conceivable that loss of GIIβ in *psl4* plants (Fig. S1*B*) greatly decreases the α-subunit levels and thus GII activity in the ER.

This raises the possibility that the residual ER GII activity in the mutants is insufficient to maintain the amounts of recognition-competent receptor and thus full capacity to trigger downstream signaling. Elf18-induced ROS spiking is strongly reduced below detectable levels in *psl5–1* plants (Fig. 2*C*) even in the presence of a high dosage (1 μM) of the ligand (Fig. S5). Ethylene production is only slightly stimulated by elf18 (Fig. S3). However, we observed a significant increase of MAPK activity and callose deposits upon elf18 elicitation, albeit to a substantially lesser degree compared with the WT plants (Fig. 2*D*, Fig. 3, and Fig. S6*A*). We note a possible discrepancy between our results and the claim that MAPKs act upstream of ROS and callose production in the FLS2 pathway (25). In contrast, all FLS2-mediated signaling outputs tested are retained at the WT-like levels (Fig. 2 *C* and *D*, Fig. 3, and Fig. S3).

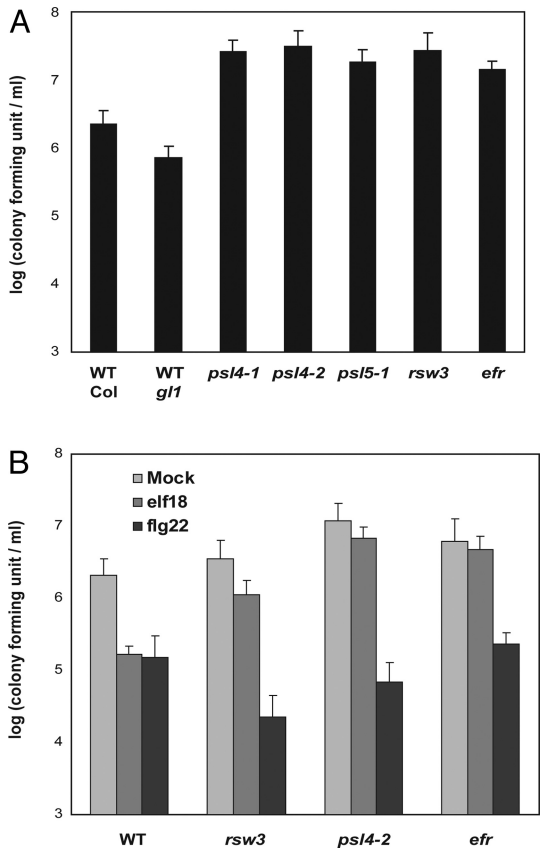

Fig. 4. Plants carrying *gII* mutations are highly susceptible to *Pst* DC3000. (*A*) Growth of *Pst* DC3000 in 4-week-old plant leaves 3 d after spray infection with bacteria at 1×10^9 cfu/mL. (*B*) MAMP-induced resistance of *gII* plants. Growth of *Pst* DC3000 3 days after infiltration with bacteria at 1×10^5 cfu/mL on 4-week-old plant leaves pretreated with 1 μM elf18, flg22, or water (i.e., mock) for 24 h. SDs are given in *A* and *B*.

In *rsw3* plants, we detected essentially intact activation of ROS and MAPKs in response to elf18 as well as flg22 (Fig. 2 *C* and *D*), although the duration of maximal elf18-induced MAPK activity might be slightly shorter than WT plants (Fig. S6). We also observed both elf18- and flg22-induced ethylene production and callose deposits (Fig. 3 and Fig. S3). Ethylene measurement revealed a WT-like elf18 dose dependence of *rsw3* plants over a 1,000-fold tested dose range (1 μM to 1 nM; Fig. S3). These results indicate that coactivation of these early and late EFR-signaling outputs is insufficient for effective repression of anthocyanin accumulation (Fig. 1 *A* and *B*). Thus, these EFR-mediated signaling outputs are uncoupled in the presence of the weakly defective *gII*α (*rsw3*) allele.

Plants Carrying Strong and Weak *gII* Mutations Are both Highly Susceptible to a Virulent Bacterial Phytopathogen. To verify the functional significance of the observed alterations in EFR-signaling outputs, we next tested the immune activity of the *gII* plants. Although previous studies have merely suspected a role of EFR in plant immunity against the virulent bacterial phytopathogen *Pseudomonas syringae* pv. *tomato* (*Pst*) DC3000 (6, 20), *efr* plants are more susceptible than WT plants to this bacterium under our assay conditions (Fig. 4*A*), in which we use a high dosage (10^9 cfu/mL) of the bacteria for spray inoculation and keep the plants under high humidity throughout the infection procedure (22) (see *Materials and Methods*). Consistent with the extensive defects in the elf18-induced responses examined, *psl4* plants clearly show high susceptibility upon challenge with *Pst* DC3000, at comparable levels to that of *efr* plants (Fig. 4*A*). Surprisingly, we detected a similar high degree of bacterial multiplication in *psl5–1* and *rsw3* plants (Fig. 4*A*), although the latter plants retain elf18-induced ROS, MAPKs, ethylene, and callose at WT-like levels (Fig. 2 *C* and *D*, Fig. 3, and Fig. S3). We infer from this *rsw3* plant phenotype that co-activation of the tested EFR-mediated signaling outputs is insufficient to mount effective defenses against the bacteria.

Elf18- but Not flg22-Induced Bacterial Resistance Is Compromised in the Weakly Defective *rsw3*/*gII*α Allele. In view of a potentially wide range of client membrane proteins that undergo GII-mediated ERQC, it is conceivable that the sum of such indirect mutational effects rather than specific defects in EFR-triggered immunity renders *rsw3* plants supersusceptible. To clarify this possibility, we next directly assessed EFR-dependent defense activity in the mutant plants. Plant pretreatment with elf18 or flg22 has been shown to reduce the multiplication of *Pst* DC3000 (20, 26) and thus provides a good indicator for MAMP-specific inducible defenses. MAMP-induced resistance was defined as the decrease in bacterial growth on elf18- and flg22-pretreated leaves as compared to water-pretreated mock leaves (Fig. 4*B*). The elf18- but not flg22-induced resistance is abolished in *efr* plants as well as in severely EFR-depleted *psl4–2* plants (Fig. 1*D*), verifying that elf18-induced resistance occurs almost entirely through EFR (Fig. 4*B*). Our analysis revealed that elf18-induced resistance is significantly impaired in *rsw3* plants, albeit to a lesser extent compared with *efr* plants, whereas fully functional flg22-induced resistance is retained (Fig. 4*B*). This strongly suggests that EFR-triggered immunity is selectively impaired in *rsw3* plants.

EFR-Mediated Transcriptional Reprogramming Is Not Sustained in *rsw3* Plants. Our results predict that *rsw3* plants are impaired at another critical step in EFR-triggered immunity than the activation of ROS, ethylene, MAPKs, and callose deposition that are generally considered as hallmarks for MTI (1). We therefore examined potential alterations in elf18-induced defense gene expression in the mutant, which would account for the immunocompromised phenotype (Fig. 4 *A* and *B*). Up-regulation of *WRKY22* and *WRKY29*, encoding members of the WRKY transcription factor family (27), occurs downstream of MAPK activation in response to different MAMPs (2, 25, 28, 29). We thus monitored expression of these genes in WT and *rsw3* seedlings during the time course of elf18 treatment. Both *WRKY* genes are rapidly induced within 1 h of elf18 application, and their transcript levels remain high over the 24-hour time course analyzed in WT plants (Fig. 5). In contrast, *rsw3* plants fail to retain elevated *WRKY* transcripts after the rapid WT-like increases within the first hour (Fig. 5). Together with the lack of a detectable peak in strongly defective *psl4–1* plants (Fig. S7), this points to the existence of initial and secondary phases in EFR signaling, of which the latter is affected in this weak *gII*α allele. The initial activation of both *WRKY* genes is in good accordance with the observed normal activation of the other early outputs, ROS, ethylene, and MAPKs (Fig. 2 *C* and *D* and Fig. S3). Thus, the observed transient nature of *WRKY* gene up-regulation suggests that sustained activation, but not initial activation, of EFR signaling is compromised in the mutant. Consistent with this, late activation of *PR1* and *PR2*, encoding defense-related proteins (30), is also impaired in response to elf18. Conversely, flg22-mediated induction of these genes is largely indistinguishable between WT and *rsw3* plants (Fig. 5), again indicating a selective perturbation of EFR function in the *gII*α allele.

Discussion

We show here that both the catalytic α-subunit and ER-retention β-subunit of GII are required for the biogenesis of functional EFR. The identification of GII together with CRT3 and UGGT in our present and parallel studies (22) has revealed several unique aspects of ERQC in plants: (*i*) A branch of the ERQC system, namely the

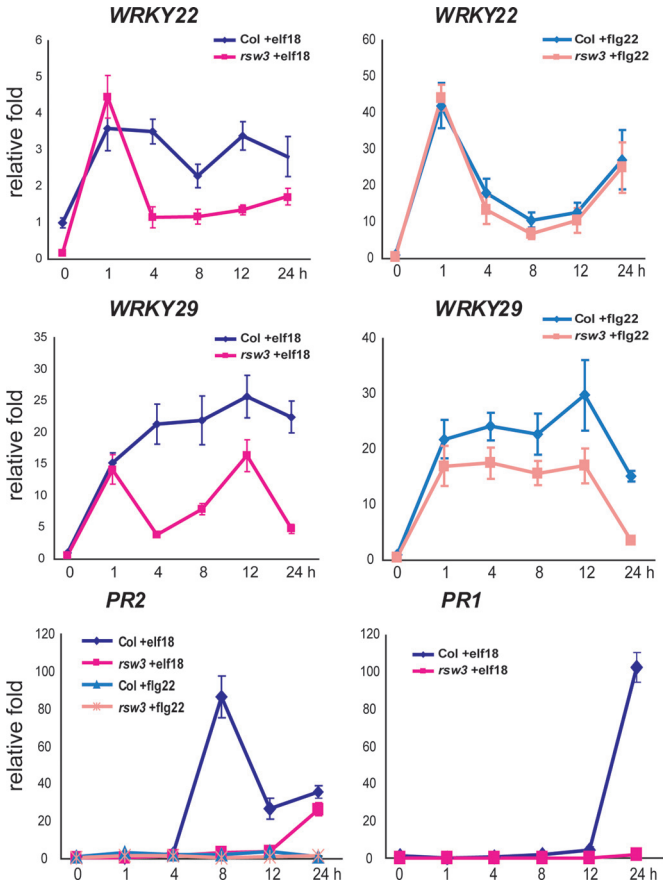

Fig. 5. Sustained transcriptional reprogramming on elf18 elicitation is compromised in *rsw3* plants. Quantitative RT-PCR analysis of 2-week-old plants treated with 1 μM elf18 or flg22 for the indicated times. The relative induction (in fold) is shown, with the *gene/ACTIN* values at 0 h in WT plants as 1. A representative data set is shown with SD of experimental replicates.

GII/CRT3/UGGT cycle, is selectively required for stable accumulation of EFR but not of a structurally related PRR, FLS2. (*ii*) Abundance control and quality control of a client receptor, EFR, is uncoupled in weakly dysfunctional *gIIα* and *crt3* alleles. (iii) EFR-mediated signaling outputs are partially and differentially, rather than uniformly, impaired in these weak alleles. This latter aspect provokes a previously unsuspected role of ERQC in the modulation of postrecognition signaling of EFR.

Our genetic analysis has revealed important features of EFR-mediated postrecognition signaling. In the presence of the *psl5–1* (*gIIα*) allele, EFR-mediated ROS spiking is below detectable levels despite substantial (albeit not full) activation of MAPKs and callose deposition (Fig. 2 *C* and *D* and Fig. 3). Conversely, in *psl1–1* (*crt3*) plants, EFR-mediated ROS spiking occurs at slightly lower levels than in WT plants despite nearly background-level activation of MAPKs and callose (22). These results either contradict the notion deduced from FLS2-mediated signaling that MAPKs act upstream of ROS spiking (25) or suggest possible differences in the sequential order of postrecognition signaling events initiated by EFR and FLS2. More importantly, our data disfavor a simple threshold model in which, e.g., more EFR signaling fluxes are required for callose deposition than ROS spiking, as rejected in the *psl5–1* plants earlier. Rather, our data would favor a notion, at least in the case of EFR, that these diverse signaling outputs are under the control of separate signaling pathways. Lowered capacity of the GII/CRT3/UGGT cycle would no longer allow EFR to govern the whole signaling processes. A strong correlation is apparent between the retained ligand binding capacity and retained signaling outputs in those *gIIα* and *crt3* alleles (Fig. S4*B*) (22). Considering the client receptor topology, it would be the LRR domain that undergoes ERQC in the ER lumen and then is exposed to the outer surface of the plasma membrane. The folding quality of this presumed ligand binding domain of EFR might determine its downstream signaling activity.

Substantial defects in EFR-triggered immunity (Fig. 4*B*) despite essentially full co-activation of ROS, MAPKs, ethylene production, and callose deposition in *rsw3* plants (Fig. 2 *C* and *D*, Fig. 3, and Fig. S3) hint at the existence of another as yet undefined key step in MTI. It has been assumed that the aforementioned hallmark outputs of PRR signaling collectively play a central role in MTI signaling (1). In principle, our data do not disprove this, but propose a mechanism beyond this concept. We note that EFR-triggered immunity is significantly lowered, yet not abolished, in *rsw3* plants (Fig. 4*B*). This residual elf18-induced resistance is well correlated with the observed coactivation of the 4 signaling outputs, thereby merely disproving that co-activation of these outputs contributes to MTI. Besides the anthocyanin derepression (Fig. 1 *A* and *B*), we present evidence that sustained, but not initial, elf18-induced up-regulation of *WRKY22* and *WRKY29* genes that encode defense-promoting transcription factors (2) is impaired in the *gIIα* plants (Fig. 5). Furthermore, late induction of 2 genes encoding pathogenesis-related proteins is also impaired in the mutant (Fig. 5). These defects in EFR signaling would at least in part account for the observed supersusceptibility to *Pst*.

Our findings highlight a separation in the presence of the weak *gIIα* allele between the initial induction phase and subsequent sustained activation and/or signal amplification phase of EFR-mediated signaling. However, the striking defects in the latter phase become apparent in *rsw3* plants between 1 and 4 h (Fig. 5), whereas callose deposition is retained even 24 h after elf18 elicitation (Fig. 3). This again suggests the existence of parallel and/or multi-branched signaling pathways emanating from EFR in WT plants, of which a subset cannot be maintained in an active state in the mutant. EFR produced in *rsw3* plants might be unable to sustain and/or strengthen defense signaling, possibly because of improper subcellular partitioning, less ligand sensitivity, less stability of the activated receptor per se and/or presumed receptor complex assemblies (31, 32), or combinations thereof. The importance of sustained PRR activation for effective MTI is also supported by the existence of bacterial effectors that directly suppress PRR function (33, 34), given that initial PRR activation should precede the actions of these effectors in the host cell. At present we cannot exclude that the separation between the initial and sustained MTI activation phases occurs at the level of another GII client protein(s) than EFR that acts in its signaling pathway(s). However, such client(s) must be dispensable for FLS2 signaling, given no detectable defects in FLS2-triggered immunity (Fig. 4*B*) and FLS2 signaling outputs (Fig. 1 *A* and *B*, Fig. 2 *C* and *D*, Fig. 3, and Fig. S3) in *rsw3* plants.

Finally, our data point to the potential significance of sustained MAMP receptor activation that maintains transcriptional reprogramming at a relatively late phase in mounting robust immunity. This sustained activation and/or signal amplification phase might involve the actions of MAMP-induced salicylic acid (35, 36) and/or weak activation of resistance proteins (37).

Materials and Methods

Plant Materials and Growth Conditions. Arabidopsis M2 population used for *psl* mutant screening is in the Col-0 *glabrous1* (*gl1*) mutant background (Lehle Seeds). *efr-1* and *fls2* mutants have been described previously (20, 26). The WT control used was Col-0 unless otherwise stated. For the sucrose-MAMP crosstalk assays, seedlings were grown under constant light in liquid medium containing 0.5× MS for 3 d and then for a further 3 d with or without the addition of 100 mM sucrose and MAMPs at the indicated concentrations. For MAPK/callose and gene expression assays, seedlings were grown on 0.5× MS agar plates or liquid me-

dium, respectively, with 25 mM sucrose under 12 h light/12 h dark conditions for 10 to 14 d. Plants were grown on soil under 10 h light/14 h dark conditions for 4 to 5 weeks for ROS and bacterial inoculation assays.

Bioassays for MAMP-Induced Responses. Anthocyanin content in whole seedlings was determined as described (38), using at least 3 sets of more than 8 seedlings per treatment. ROS assays were performed essentially as described previously (5) with the following modifications. Leaf discs (5 mm diameter) excised from mature leaves were kept on water overnight before the luciferase-based measurement of ROS generation triggered by the addition of MAMPs at 100 nM unless otherwise stated. For MAPK and gene expression assays, the whole seedlings were applied with elf18 or flg22 at 1 μM for the indicated times. MAPK activation was detected by immunoblot analysis of soluble proteins extracted from the seedlings in a lysis buffer described previously (39) using anti-phospho p44/p42 MAPK antibody. For callose induction, elf18 and flg22 were applied at 2 or 1 μM for 24 h, respectively. Callose deposits were stained with aniline blue and visualized as described (40). The MAMP concentrations used were optimized for consistent detection of differences between WT and corresponding receptor mutant (*efr* or *fls2*) plants: robust MAMP responses were hardly detectable without high variations in WT plants below the concentrations used under our conditions.

Pathogen Inoculation and Growth Assays. Bacterial inoculation assays were preformed as described previously (26) with the following modifications. *Pst* DC3000 was sprayed onto leaf surface at 1×10^9 cfu/mL. Infected plants were kept in a covered container for 3 d before harvesting leaves. A total of 12 surface-sterilized leaf discs (5 mm diameter) excised from 2 leaves of 6 plants per genotype were randomly separated into 3 pools, and then subjected to the quantification of leaf bacteria. For MAMP-induced resistance assays, plants were syringe-infiltrated with 1 μM elf18, flg22, or water (i.e., mock) 24 h before inoculation. *Pst* DC3000 suspension at 1×10^5 cfu/mL was syringe-infiltrated into 2 to 3 leaves of 8 plants per genotype per treatment. Three days after inoculation, a leaf disc (5 mm diameter) was excised from 12 representative leaves per treatment. These 12 leaf discs were separated into 3 pools and then used to determine bacterial titers. These experiments have been repeated 3 times with the same conclusion.

ACKNOWLEDGMENTS. We thank Dr. Imre Somssich for useful comments on the manuscript; and Dr. Steffen Rietz, Heidrun Häweker, Maret-Linda Kalda, Brigitte Pickel, and Eva-Maria Reimer for technical assistance. The T-DNA insertion line (*psl4–2*) and *rsw3* seeds were provided by the Arabidopsis Biological Resource Center. This work was supported in part by the Max Planck Society, grants from SFB670 (P.S.-L. and S.R.), and PhD fellowships from the International Max Planck Research School Program (X.L. and N.T.).

1. Boller T, Felix G (2009) A renaissance of elicitors: Perception of microbe-associated molecular patterns and danger signals by pattern-recognition receptors. *Annu Rev Plant Biol* 60:379–406.
2. Asai T, et al. (2002) MAP kinase signalling cascade in Arabidopsis innate immunity. *Nature* 415:977–983.
3. Clay NK, Adio AM, Denoux C, Jander G, Ausubel FM (2009) Glucosinolate metabolites required for an Arabidopsis innate immune response. *Science* 323:95–101.
4. Felix G, Duran JD, Volko S, Boller T (1999) Plants have a sensitive perception system for the most conserved domain of bacterial flagellin. *Plant J* 18:265–276.
5. Gomez-Gomez L, Felix G, Boller T (1999) A single locus determines sensitivity to bacterial flagellin in Arabidopsis thaliana. *Plant J* 18:277–284.
6. Kunze G, et al. (2004) The N terminus of bacterial elongation factor Tu elicits innate immunity in Arabidopsis plants. *Plant Cell* 16:3496–3507.
7. Asselbergh B, De Vleesschauwer D, Hofte M (2008) Global switches and fine-tuning-ABA modulates plant pathogen defense. *Mol Plant Microbe Interact* 21:709–719.
8. Lozoya E, Block A, Lois R, Hahlbrock K, Scheel D (1991) Transcriptional repression of light-induced flavonoid synthesis by elicitor treatment of cultured parsley cells. *Plant J* 1:227–234.
9. McLusky SR, et al. (1999) Cell wall alterations and localized accumulation of feruloyl-3′-methoxytyramine in onion epidermis at sites of attempted penetration by Botrytis allii are associated with actin polarisation, peroxydase activity and suppression of flavonoid biosynthesis. *Plant J* 17:523–534.
10. Shirasu K (2009) The HSP90-SGT1 chaperone complex for NLR immune sensors. *Annu Rev Plant Biol* 60:139–164.
11. Ye Z, Ting JP-Y (2008) NLR, the nucleotide-binding domain leucine-rich repeat containing gene family. *Curr Opin Immunol* 20:3–9.
12. Anelli T, Sitia R (2008) Protein quality control in the early secretory pathway. *EMBO J* 27:315–327.
13. Hebert DN, Molinari M (2007) In and out of the ER: Protein folding, quality control, degradation, and related human diseases. *Physiol Rev* 87:1377–1408.
14. Pattison RJ, Amtmann A (2009) N-glycan production in the endoplasmic reticulum of plants. *Trends Plants Sci* 14:92–99.
15. Boisson M, et al. (2001) Arabidopsis glucosidase I mutants reveal a critical role of N-glycan trimming in seed development. *EMBO J* 20:1010–1019.
16. Burn JE, et al. (2002) The cellulose-deficient Arabidopsis mutant rsw3 is defective in a gene encoding a putative glucosidase II, an enzyme processing N-glycans during ER quality control. *Plant J* 32:949–960.
17. Gillmor CS, Poindexter P, Lorieau J, Palcic MM, Somerville C (2002) Alpha-glucosidase I is required for cellulose biosynthesis and morphogenesis in Arabidopsis. *J Cell Biol* 156:1003–1013.
18. Koiwa H, et al. (2003) The STT3a subunit isoform of the Arabidopsis oligosaccharyltransferase controls adaptive responses to salt/osmotic stress. *Plant Cell* 15:2273–2284.
19. Gomez-Gomez L, Boller T (2000) FLS2: An LRR receptor-like kinase involved in the perception of the bacterial elicitor flagellin in Arabidopsis. *Mol Cell* 5:1003–1011.
20. Zipfel C, et al. (2006) Perception of the bacterial PAMP EF-Tu by the receptor EFR restricts Agrobacterium-mediated transformation. *Cell* 125:749–760.
21. Gould KS, Lister C (2006) Flavonoid functions in plants. *Flavonoids: Chemistry, Biochemistry, and Applications*, eds Andersen ØM, Markham KR (CRC Press, Boca Raton, FL), pp 397–441.
22. Saijo Y, et al. (2009) Receptor quality control in the endoplasmic reticulum for plant innate immunity. *EMBO J* 28:3439–3449.
23. Trombetta ES, Fleming KG, Helenius A (2001) Quaternary and domain structure of glycoprotein processing glucosidase II. *Biochemistry* 40:10717–10722.
24. Trombetta ES, Simons JF, Helenius A (1996) Endoplasmic reticulum glucosidase II is composed of a catalytic subunit, conserved from yeast to mammals, and a tightly bound noncatalytic HDEL-containing subunit. *J Biol Chem* 271:27509–27516.
25. Zhang J, et al. (2007) A Pseudomonas syringae effector inactivates MAPKs to suppress PAMP-induced immunity in plants. *Cell Host Microbe* 1:175–185.
26. Zipfel C, et al. (2004) Bacterial disease resistance in Arabidopsis through flagellin perception. *Nature* 428:764–767.
27. Shen QH, et al. (2007) Nuclear activity of MLA immune receptors links isolate-specific and basal disease-resistance responses. *Science* 315:1098–1103.
28. Libault M, Wan JR, Czechowski T, Udvardi M, Stacey G (2007) Identification of 118 Arabidopsis transcription factor and 30 ubiquitin-ligase genes responding to chitin, a plant-defense elicitor. *Mol Plant-Microbe Interact* 20:900–911.
29. Navarro L, et al. (2004) The transcriptional innate immune response to flg22. Interplay and overlap with Avr gene-dependent defense responses and bacterial pathogenesis. *Plant Physiol* 135:1113–1128.
30. van Loon LC, Rep M, Pieterse CMJ (2006) Significance of inducible defense-related proteins in infected plants. *Annu Rev Phytopathol* 44:135–162.
31. Chinchilla D, et al. (2007) A flagellin-induced complex of the receptor FLS2 and BAK1 initiates plant defence. *Nature* 448:497–500.
32. Heese A, et al. (2007) The receptor-like kinase SERK3/BAK1 is a central regulator of innate immunity in plants. *Proc Natl Acad Sci USA* 104:12217–12222.
33. Xiang T, et al. (2008) Pseudomonas syringae effector AvrPto blocks innate immunity by targeting receptor kinases. *Curr Biol* 18:74–80.
34. Göhre V, et al. (2008) Plant pattern-recognition receptor FLS2 is directed for degradation by the bacterial ubiquitin ligase AvrPtoB. *Curr Biol* 18:1824–1832.
35. Mishina TE, Zeier J (2007) Pathogen-associated molecular pattern recognition rather than development of tissue necrosis contributes to bacterial induction of systemic acquired resistance in Arabidopsis. *Plant J* 50:500–513.
36. Tsuda K, Sato M, Glazebrook J, Cohen JD, Katagiri F (2008) Interplay between MAMP-triggered and SA-mediated defense responses. *Plant J* 53:763–775.
37. Kim MG, Geng X, Lee SY, Mackey D (2009) The *Pseudomonas syringae* type III effector AvrRpm1 induces significant defenses by activating the Arabidopsis nucleotide-binding leucine-rich repeat protein RPS2. *Plant J* 57:645–653.
38. Teng S, Keurentjes J, Bentsink L, Koornneef M, Smeekens S (2005) Sucrose-specific induction of anthocyanin biosynthesis in Arabidopsis requires the MYB75/PAP1 gene. *Plant Physiol* 139:1840–1852.
39. Saijo Y, et al. (2008) Arabidopsis COP1/SPA1 complex and FHY1/FHY3 associate with distinct phosphorylated forms of phytochrome A in balancing light signaling. *Mol Cell* 31:607–613.
40. Lipka V, et al. (2005) Pre- and postinvasion defenses both contribute to nonhost resistance in Arabidopsis. *Science* 310:1180–1183.